© 2015. Published by The Company of Biologists Ltd | Development (2015) 142, 1785-1793 doi:10.1242/dev.119057

RESEARCH ARTICLE

Dynamics of the slowing segmentation clock reveal alternating two-segment periodicity

Nathan P. Shih[1,*], Paul François[2], Emilie A. Delaune[3] and Sharon L. Amacher[4,‡]

ABSTRACT

The formation of reiterated somites along the vertebrate body axis is controlled by the segmentation clock, a molecular oscillator expressed within presomitic mesoderm (PSM) cells. Although PSM cells oscillate autonomously, they coordinate with neighboring cells to generate a sweeping wave of cyclic gene expression through the PSM that has a periodicity equal to that of somite formation. The velocity of each wave slows as it moves anteriorly through the PSM, although the dynamics of clock slowing have not been well characterized. Here, we investigate segmentation clock dynamics in the anterior PSM in developing zebrafish embryos using an *in vivo* clock reporter, *her1:her1-venus*. The *her1:her1-venus* reporter has single-cell resolution, allowing us to follow segmentation clock oscillations in individual cells in real-time. By retrospectively tracking oscillations of future somite boundary cells, we find that clock reporter signal increases in anterior PSM cells and that the periodicity of reporter oscillations slows to about ∼1.5 times the periodicity in posterior PSM cells. This gradual slowing of the clock in the anterior PSM creates peaks of clock expression that are separated at a two-segment periodicity both spatially and temporally, a phenomenon we observe in single cells and in tissue-wide analyses. These results differ from previous predictions that clock oscillations stop or are stabilized in the anterior PSM. Instead, PSM cells oscillate until they incorporate into somites. Our findings suggest that the segmentation clock may signal somite formation using a phase gradient with a two-somite periodicity.

KEY WORDS: Two-segment periodicity, Segmentation clock, Zebrafish, *In vivo* imaging, *her1*, Somite, Oscillations

INTRODUCTION

In vertebrates, the process of somitogenesis generates mesodermal blocks of tissue – called somites – from the undifferentiated presomitic mesoderm (PSM). Somites flank the notochord and eventually give rise to structures such as axial muscles and vertebrae. Somites are formed sequentially with regularity in size, periodicity and number within each species. Segmentation is resilient and adjusts for changes in PSM size (Lauschke et al., 2013) and temperature (Schröter et al., 2008). To account for the regularity of somite formation, Cooke and Zeeman (1976) proposed two hypothetical interacting mechanisms behind somitogenesis: a 'clock' and a 'wavefront'. They hypothesized that cells in the PSM would oscillate between a permissive and restrictive phase (clock), periodically forming somites based on their interaction with a positional signal (wavefront), the latter progressing across the embryo at the same rate as tailbud elongation. PSM cells in the permissive phase of the clock would respond to the wavefront by pinching off and rapidly transitioning from undifferentiated PSM cells into segmented somites. Their model informed the search for factors that molecularly define the clock and wavefront, and forms the basis of most somitogenesis models today (Lewis et al., 2009; Aulehla and Pourquié, 2010; Pourquié, 2011; Oates et al., 2012).

Through experimental and theoretical data across a wide breadth of organisms, the periodicity and timing of somite formation is now thought to be controlled by a molecular network known as the segmentation clock (Pourquié, 2011; Oates et al., 2012; Palmeirim et al., 1997; Holley et al., 2000; Jouve et al., 2000; Henry et al., 2002; Oates and Ho, 2002; Bessho et al., 2003). Clock genes oscillate in individual PSM cells and some of them are essential for proper somite formation. PSM cell oscillations are locally coordinated, with the Notch pathway necessary for synchronizing expression in neighboring cells (Pourquié, 2011; Oates et al., 2012). The synchronous oscillations of clock cycling generate a wave of gene expression that is propagated as a narrowing stripe from the posterior to the anterior PSM and is kinematic, produced by local, coordinated expression in individual cells rather than the bulk transport or transduction of molecules or cells. The periodicity of oscillatory expression of cyclic genes *in vivo* in the posterior PSM matches the rate of somite generation, with each wave of clock expression reaching the PSM-somite boundary as a new somite is formed (Oates et al., 2012; Aulehla et al., 2008; Masamizu et al., 2006; Takashima et al., 2011; Delaune et al., 2012), although recent work shows that oscillation and segmentation periodicities are offset during tail segmentation (Soroldoni et al., 2014).

A family of core clock components has been shown to oscillate within the vertebrate PSM: the Hairy/Enhancer-of-split (*Hes*) transcriptional repressors (Palmeirim et al., 1997; Jouve et al., 2000; Bessho et al., 2001). The cycling of these *hairy*-related genes was first deduced in fixed embryos by *in situ* hybridization. Fixing the halves of each embryo at different times or exposing each half to different temperatures revealed stripes of gene expression with a period matching that of somite formation repressors (Palmeirim et al., 1997; Jouve et al., 2000; Jiang et al., 2000). In zebrafish, *hairy/enhancer-of-split*-related (Her) genes, *her1* and *her7*, have been shown to oscillate in the PSM and are necessary for proper somite formation (Pourquié, 2011; Oates et al., 2012; Henry et al., 2002; Oates and Ho, 2002). High-resolution *in situ* hybridization for Her genes show that clock expression sweeps in a posterior-to-anterior direction: in each stripe of expression, transcripts in the more posterior edge of the stripe are localized in the cytosol, whereas cells in the anterior have transcripts localized in nuclear puncta (Jülich et al., 2005; Mara et al., 2007; Giudicelli et al., 2007). Recently, we directly observed waves of zebrafish cyclic gene

[1]Department of Molecular and Cell Biology, University of California, Berkeley, CA 94720, USA. [2]Department of Physics, McGill University, Montréal, Canada H3A 2T8. [3]UMR 5305 CNRS/UCBL, 7 passage du Vercors, Lyon 69367, Cedex 07, France. [4]Departments of Molecular Genetics and Molecular and Cellular Biochemistry, The Ohio State University, Columbus, OH 43210, USA.
*Present address: Department of Biomedical Engineering, University of California, Davis, CA 95616, USA.

‡Author for correspondence (amacher.6@osu.edu)

Received 23 October 2014; Accepted 19 March 2015

Development (2015) 142, 1785-1793 doi:10.1242/dev.119057

expression using a single-cell resolution clock reporter, *her1:her1-venus*, in which the 8.6-kb *her1* regulatory region drives expression of a transcript encoding a Her1-Venus fusion protein, flanked by *her1* 5′- and 3′-UTRs to facilitate rapid transcript turnover (Delaune et al., 2012). Using this reporter, we described the behavior of oscillating cells at a local level, confirming that the Notch pathway synchronizes neighboring cells and revealing that daughter cells oscillate synchronously after mitosis. The *her1:her1-venus* reporter is thus a powerful tool to explore how segmentation clock signal is translated to pattern each forming somite.

In both fixed and live embryos, the cyclic gene expression wave slows as it approaches the anterior PSM, a feature not described in the original clock and wavefront model (Cooke and Zeeman, 1976; Delaune et al., 2012). As more data were gathered about the slowing of clock gene oscillations, models have been proposed to explain how this slowing influences segment formation. The function of clock slowing is still unclear; recent models suggested the clock freezes as it interacts with a theoretical ‘arrest front’, effectively stopping and stabilizing clock expression (Oates et al., 2012; Giudicelli et al., 2007; Morelli et al., 2009; Herrgen et al., 2010). The observed clock slowing would then account for the continuous transition from a finite period in the tail bud to an ‘infinite period’ at the front. Some calculations based on clock oscillations in mice suggest that clock expression does not stabilize in the anterior PSM, but may only slow to a 1.5-segment periodicity (Niwa et al., 2011). Importantly, transition from oscillating systems to somites does not require *a priori* a diverging period (François and Siggia, 2012). Understanding how the clock behaves in the anterior PSM may have important implications in understanding somite patterning and will also inform somitogenesis models, ensuring that models accurately reflect phenomena observed in the developing embryo. For example, the dynamics of clock slowing could help to determine where somite boundaries and/or somite polarity are patterned.

Here, we follow oscillating PSM cells *in vivo* to investigate the slowing of the clock relative to somite boundary formation. We focus on cells that eventually form each somite boundary, using the *her1:her1-venus* reporter to examine clock oscillation patterns in future boundary cells through developmental time. We find that the clock initially oscillates in the posterior PSM with a periodicity that matches the rate of somitogenesis, gradually slows as PSM cells become more anterior, and increases in amplitude during the final two oscillations. The clock slowing in anterior PSM cells creates a phase distribution where cells at a one-somite distance are actually in opposite phases of clock expression. Importantly, we do not find evidence for an arrest front that would cause clock expression to drastically increase in period as it stops or stabilizes in the anterior PSM, ceasing oscillations. Based on these results, we propose an updated interpretation of how the segmentation clock patterns somites.

RESULTS

To understand the dynamics of clock slowing and the relationship of slowing to somite formation, we followed oscillations in cells progressing anteriorly in the PSM. We tracked cells over time in the transgenic line *her1:her1-venus*, a single-cell resolution clock reporter (Delaune et al., 2012), focusing on cells that will eventually constitute each somite boundary. Zebrafish embryos were injected at one-cell stage with *h2b-cerulean* and *lyn-mcherry* mRNA to mark nuclei and membranes, respectively (Delaune et al., 2012; Megason, 2009). The PSM was imaged beginning at the 10-12 somite stage for 4-6 h and PSM cells were tracked through time using a semi-automated cell tracking software (Delaune et al., 2012). As in our previous study (Delaune et al., 2012), we imaged embryos at 23°C to lengthen the somitogenesis period (Schröter et al., 2008) and allow for more time to image embryos. Each peak of expression was correlated to the approximate anterior-posterior global position of the cell in the PSM and its position relative to the most recently formed somite. We used conventions in the field (Pourquié and Tam, 2001), with the newest fully-formed somite named S1 and the second-newest formed somite named S2. The region constituting the forming somite is named S0, while regions forming the two subsequent future somites are named S-1 and S-2, respectively (Fig. 1A). To identify the oscillations of each cell relative to its final oscillation, we propose a nomenclature that is similar to that of somitogenesis: the final oscillation peak of a given cell is named ‘P0’, while the second to last is named ‘P-1’, third to last ‘P-2’, and so forth. As previously noted by us and others, we observed that reporter oscillations are faster in posterior PSM cells than in anterior ones, and that reporter expression levels in anterior PSM cells are larger in amplitude than in posterior PSM cells (Fig. 1B,C) (Ay et al., 2014; Lauschke et al., 2013; Delaune et al., 2012). We quantified the periodicity of oscillations by measuring the time between each peak of fluorescence and normalizing it to the somitogenesis period. All peaks of oscillations were identified by both raw fluorescence measurements and calculated sinusoidal waves using a validated smoothing heuristic (Delaune et al., 2012). As expected, cells in the posterior PSM oscillate with a periodicity that approximately matches somitogenesis (Fig. 1D, ‘P-5’ to ‘P-3’) (Delaune et al., 2012; Oates et al., 2012; Holley et al., 2000; Giudicelli et al., 2007). The periodicity increases in a linear fashion as cells progress anteriorly, with a 50.7% longer period (s.e.m.=1.2%) between P0 and P-1 (Fig. 1D) compared with the periodicity of somitogenesis. We do not see evidence of period divergence to infinity, contrary to suggestions in previous models (Oates et al., 2012; Giudicelli et al., 2007; Morelli et al., 2009; Herrgen et al., 2010). We also quantified the increase in amplitude of clock expression in the last two oscillations of anterior PSM cells (Fig. 1E). Clock expression in the posterior PSM has little or no change in amplitude when compared with the previous oscillation (Fig. 1E, ‘P-5’ to ‘P-3’). However, we noted a 58.9±3.6% increase in fluorescence in comparing the second-to-last oscillation with the third-to-last oscillation (‘P-2’ versus ‘P-1’), and an additional 70.1±4.6% increase when comparing the last oscillation with the second-to-last (Fig. 1E, ‘P-1’ versus ‘P0’). The gradual signal increase and slowing of the clock was observed in all PSM cells (four embryos, 243 cells), regardless of the final position of the cell within a formed somite.

With cells in the posterior PSM oscillating with the same periodicity as somitogenesis, one wave of clock expression is propagated through the PSM for each somite formed. As the clock slows, these waves condense into narrowing peaks of expression. Current models of somitogenesis routinely position peaks of clock signal at one-somite length intervals in the anterior PSM, where period eventually diverges towards infinity at the PSM-somite boundary (Oates et al., 2012; Giudicelli et al., 2007; Morelli et al., 2009; Herrgen et al., 2010). To examine the dynamics of clock slowing in the anterior PSM, we followed reporter expression over time in cells that eventually form either side of somite boundaries (Fig. 2A,A′). We found that oscillations in anterior boundary cells of the forming somite (cells circled in red, Fig. 2A′) are nearly synchronous to cells in the adjacent posterior boundary of the previously formed somite (circled in blue, Fig. 2A′,B). A prominent distinction between these two neighboring populations is that cells in the anterior S0 will oscillate one more time compared with the

Development (2015) 142, 1785-1793 doi:10.1242/dev.119057

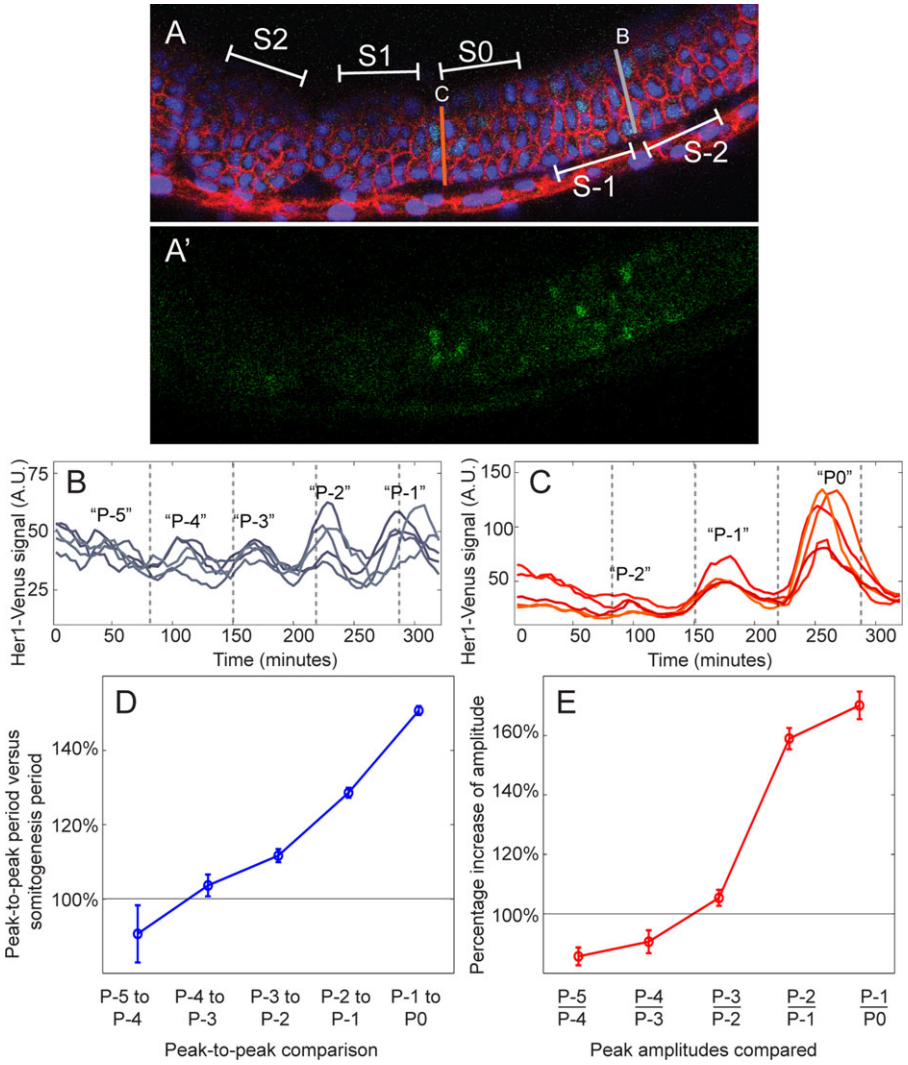

Fig. 1. Clock expression in anterior PSM cells gradually slows and increases in amplitude over the last two oscillations. (A) Representative embryo indicating somite designations in PSM and developing somites, with regions delineating formed somites (S1, S2), forming somite S0 and future somites (S-1, S-2) indicated. Gray and orange lines denote the approximate positions of cells at the last timepoint in B and C, respectively. Labeling of the nucleus and cell membrane is indicated by H2B-Cerulean (blue) and lyn-mCherry (red), respectively (A), and Her1-Venus reporter fluorescence is shown in green (A′). (B,C) Single-cell clock oscillations in a group of five neighbors in the posterior PSM (B) and the anterior PSM (C). Number of clock oscillations remaining is included in quotes above the expression peaks, with 'P0' indicating the last oscillation peak, 'P-1' indicating the second-to-last oscillation peak, and so on. The 'P0' oscillation peak occurs within S-1 or S0, depending on their final position in the forming somite (Delaune et al., 2012). Gray dashed lines indicate the times at which morphological somite boundaries are visibly formed. (D) The periodicity of clock expression relative to the periodicity of somitogenesis. Periodicity of oscillations was measured in four embryos (n=243 cells) based on the time between peaks of maximum expression. Somite periodicity was calculated based on the timing of morphological alignment of the boundary cells. (E) The change in clock expression amplitude measured in four embryos (n=243 cells), based on the ratio of amplitude change between two sequential oscillations. Data are mean±s.e.m.

cells incorporated into posterior S1, which cease to oscillate. The last oscillation of S1 posterior boundary cells appears similar to the adjacent S0 anterior boundary cells, ceasing oscillations without becoming fixed in a persistently 'on' or 'off' state. We observed the same pattern in boundary cells that formed the previously formed somite (circled as green and orange in Fig. 2A′): synchronous oscillations, with cells that form the future anterior S1 boundary oscillating one more time after boundary cells that form the future posterior S2 boundary have stopped oscillating (Fig. 2D). Mitosis in the PSM produces daughters that oscillate in tight synchrony (Delaune et al., 2012); if the characteristic 'extra' cycle is a robust feature of neighboring cells that join adjacent somites, we expected to observe that pattern in highly synchronized daughters, but only if they eventually contribute to opposite sides of a somite boundary. In a rare example where cell division occurred early enough to allow tracking and the daughters separated enough to join adjacent somites, that is exactly the pattern observed (supplementary material Fig. S1). Finally, our cell-tracking analyses also reveal that cells that incorporate into a posterior somite boundary cease oscillations prior to cells that incorporate into the anterior boundary of the same somite [Fig. 2B-E, compare anterior S1 cells (green) with posterior S1 cells (blue); supplementary material Fig. S2], contrary to what is predicted by current models. Thus, within the same presumptive somites, clock oscillations stop from a posterior-to-anterior direction, without any 'freezing' of the phase or period divergence (Fig. 2B-E; supplementary material Fig. S2). This is in contrast to clock and wavefront models where the clock is expected to stop from an anterior-to-posterior direction following continuous wavefront dynamics (Oates et al., 2012; Giudicelli et al., 2007; Morelli et al., 2009; Herrgen et al., 2010).

Development (2015) 142, 1785-1793 doi:10.1242/dev.119057

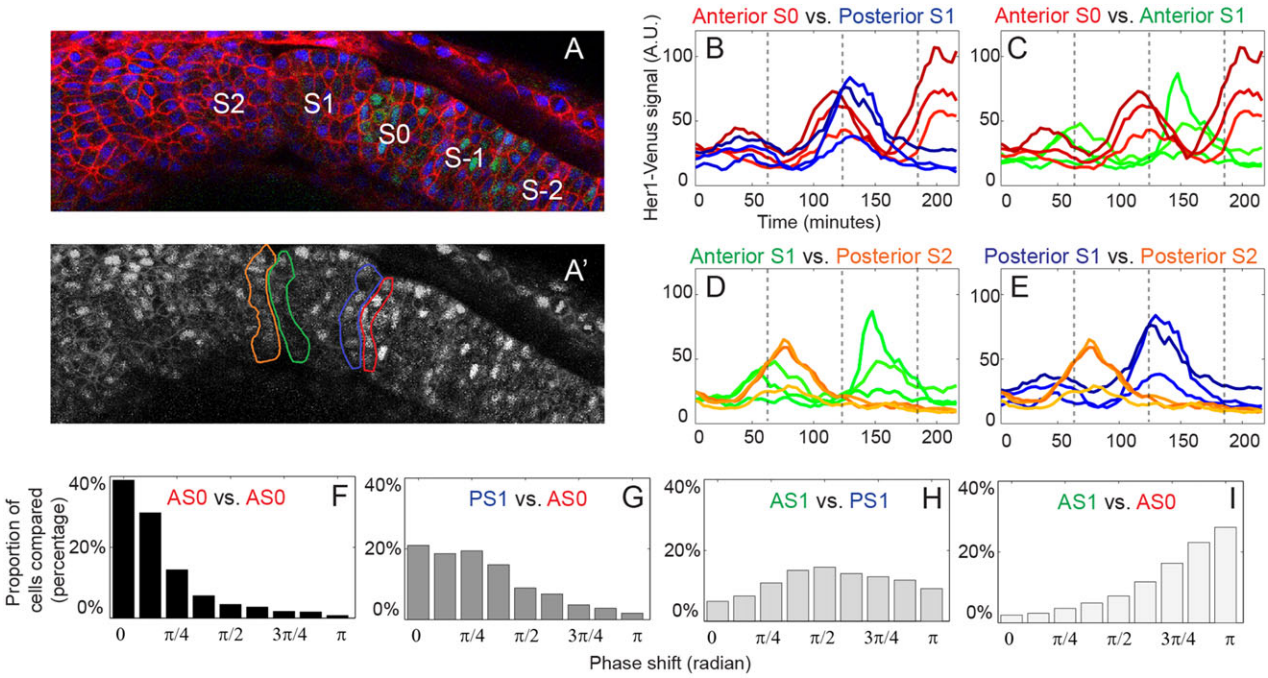

Fig. 2. Neighboring anterior PSM cells oscillate synchronously regardless of final somite position, while cells at a one-somite distance are in anti-phase. (A) Embryo at one timepoint (220 min, in B-E) during a time lapse. Her1-Venus reporter fluorescence is indicated in green, with nuclei and membrane labeled with H2B-Cerulean and lyn-mCherry, respectively. (A′) Black and white image of the embryo in A. Colored outlines indicate the cohort of cells used to represent each boundary. S0 and S1 boundary cohorts (red/blue and orange/green, respectively) were identified by retrospectively tracing actual boundary cells. (B-E) Raw reporter fluorescence levels of three representative cells from each boundary cohort indicated in A′. To indicate the periodicity of somite formation, gray dashed lines indicate times at which morphological somite boundaries are forming in the imaged embryo. (F-I) Histograms of phase differences between boundary cell cohorts. Comparisons are made at every timepoint in the timelapse, and cells were identified based on their position at the end of the timelapse. Comparisons were made only if both cells were still oscillating. Phase differences are plotted between 0 (indicating cells are exactly in phase) and π (indicating opposite phase). Distance between the two compared populations increases from left to right. Average phase differences are 0.75 (F), 1.12 (G), 1.59 (H) and 2.17 (I), calculated from 15,003-35,740 pairwise comparisons in four embryos. See also supplementary material Figs S1-S3.

As mentioned above, previous work suggested that oscillations of cells one-somite length away should be synchronized in the anterior PSM (Oates et al., 2012; Giudicelli et al., 2007; Morelli et al., 2009; Herrgen et al., 2010). As expected, we find that posterior PSM cells oscillate in synchrony, even when at a one-somite distance (supplementary material Fig. S3). However, in the anterior PSM, cells that will form the anterior border of S0 have opposite levels of expression compared with cells that will form the anterior-most border of S1 (Fig. 2C): i.e. when presumptive anterior border S0 cells have peak expression levels, presumptive anterior border S1 cells are at the expression trough, and vice versa. This distinct anti-phase relationship is observed when comparing any two groups of anterior PSM cells separated by a one-somite length, including cells that incorporate into the posterior-most border (Fig. 2E) or center of formed somites (not shown). These oscillation relationships among PSM cells were consistent at every forming somite boundary we examined (15 boundaries across five embryos): cells at a one-somite distance initially oscillate in synchrony in the posterior PSM, but as the clock slows in the anterior PSM, they shift into anti-phase so that adjacent waves of cyclic expression are not synchronized in the anterior PSM.

To compare globally anterior PSM oscillation phase across multiple boundaries and embryos, we quantified the synchrony of these anterior PSM cells, using methods described previously (Delaune et al., 2012). Briefly, we used a smoothing heuristic to estimate the oscillations and clock phase of each cell at each timepoint; phase calculations were then used to quantify the phase difference between any two cells at any given timepoint as long as both cells were still oscillating (Delaune et al., 2012). Tracked cells were indexed based on their final position within a developing somite, either at the anterior or posterior border. The phases of cells constituting each boundary were compared with each other in a combinatorial fashion, calculating phase differences between cells in each group at every timepoint. Cells in the same compartment exhibited a high level of synchrony with very little phase difference between cells at any given time point (35,740 comparisons across four embryos, Fig. 2F). As expected, cells on either side of a somite boundary are slightly less synchronized than cells on the same side of a somite boundary (17,353 comparisons across four embryos, Fig. 2G). Across a larger distance, clock synchrony in the anterior PSM continues to decrease (15,003 comparisons across four embryos, Fig. 2H), with maximum phase difference at one-somite length away (25,326 comparisons across four embryos, Fig. 2I). These data validate previous observations that cells in close proximity are synchronized (Delaune et al., 2012), and we show here that a somite boundary does not create an exception to that finding. Instead, a gradual phase gradient is distributed along the length of the anterior PSM, with adjacent cells oscillating in phase and cells at a one-somite distance in anti-phase.

To gain a better sense of how clock oscillations behave throughout the entire PSM, we performed a tissue-level analysis of clock behavior, retrospectively examining populations of cells based on their final position in the developing embryo. By broadly analyzing the waves of clock expression across space and time, we searched for repeating patterns of clock oscillations that match the repeated formation of somites. Using automated scripts (see

Development (2015) 142, 1785-1793 doi:10.1242/dev.119057

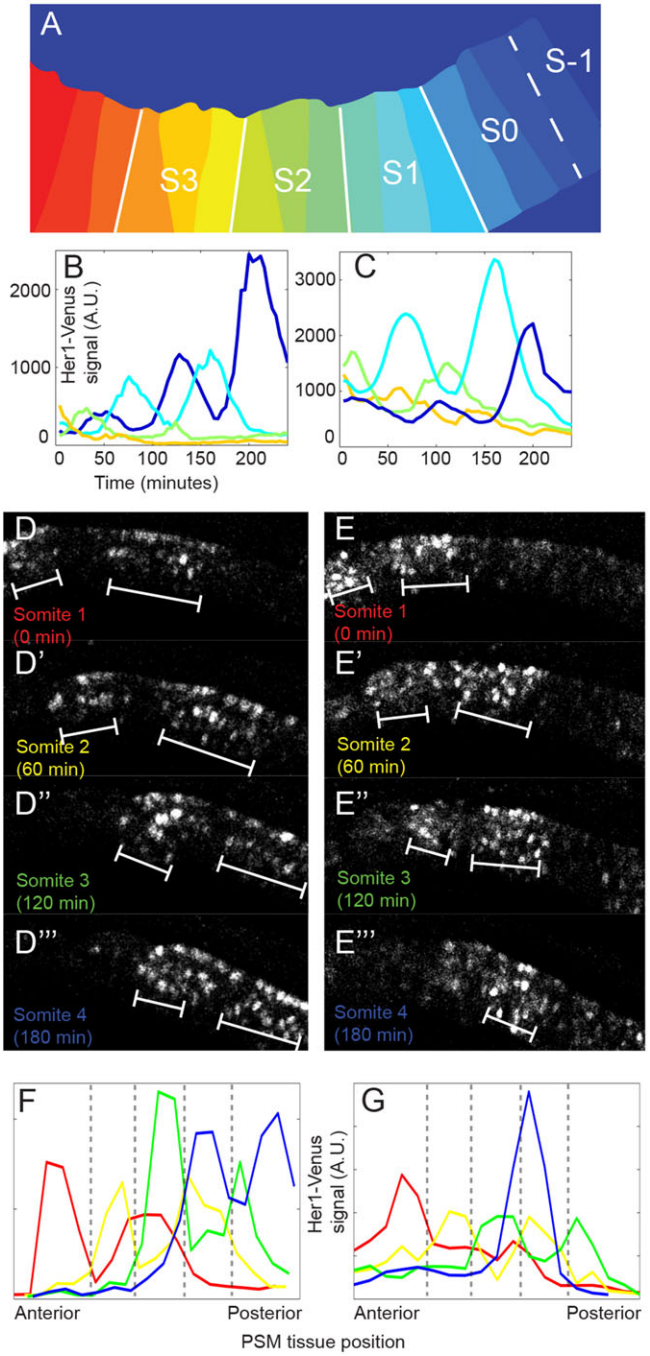

Fig. 3. In the anterior PSM, clock oscillations have a two-somite periodicity. (A) An example of PSM tissue separated into sectors for tissue-level fluorescence measurements that depicts a representative endpoint for traces shown in B and C. Tissue fluorescence was measured using the center one-third of each future somite to ensure fluorescence measurements were representative of only one somite. White lines denote the position of somite boundaries at the end of the timelapse. (B,C) Tissue-wide fluorescence quantification in two representative embryos. Total fluorescence in the center slice of each future somite and S0 is plotted through time until the somite forms. Line color matches stripe position in A. Tissue-level fluorescence amplitude quantification is noisier for cell groups oscillating near the baseline, and trends observed when following single cells (e.g. last peak having highest amplitude) are not always recapitulated when tissue-level peaks and troughs are close to the baseline (e.g. green traces). (D,E) Raw fluorescence confocal image of Her1-Venus signal (a merge of five consecutive *z*-stacks) in two different embryos. Images shown are PSM 'snapshots' taken just as a somite is forming more anteriorly, based on morphological landmarks. White brackets denote areas of highest clock reporter expression. (F,G) Clock reporter levels were quantified across the PSM at each timepoint shown in D-D‴ and E-E‴, respectively, and then mapped collectively onto a reference PSM. Line color corresponds to labeling in D-D‴ and E-E‴. Gray dashed lines mark morphological somite boundaries (which appear later). See also supplementary material Fig. S4.

Materials and Methods), *z*-stacks of images at each timepoint were processed to detect the axis of the embryo based on injected nuclear and membrane labels. We divided the somite and PSM tissue into sectors at the end of each timelapse – with each future somite delineated into thirds (Fig. 3A) – and then retrospectively measured the total combined fluorescence within cells of each sector at each timepoint. The clock expression pattern in each presumptive somite recapitulated our single-cell observations: in the anterior PSM, sectors of tissue separated by a one-somite distance were in anti-phase with each other and cells that were separated at a distance of two somites were in phase with each other (two embryos shown, Fig. 3B,C).

An embryo-wide profile of clock expression dynamics generated by measuring reporter fluorescence across the entire AP axis (without individual cell tracking) resembles the spatial readout of mRNA levels using *in situ* hybridization. However, our system measures spatial expression profiles at multiple time points over the course of development in a single embryo rather than at a single timepoint in a fixed embryo, and provides a correlation across the presomitic mesoderm between clock dynamics and eventual somitic fate. Tissue-wide fluorescence was quantified by totaling reporter signal within each digital sector of PSM. Based on morphological furrowing of somite boundaries, we examined fluorescence reporter levels in the PSM at each moment a somite was forming (Fig. 3D-E‴). At each timepoint, we observed peaks of expression in the forming somite (S0) and at a two-somite distance (S-2), with minimal clock expression at the S-1 position (Fig. 3F, G). This pattern recapitulates the two stripes of expression seen in fixed embryos, with an alternating gap of gene expression between the newly forming S0 and the subsequent S-2. As the cells in S0 form a somite, cells that were previously in the S-1 position are now in S0. The pattern repeats, with cells in the new S0 and S-2 peaking in expression, while S-1 cells (halfway between these two peaks) are at a minimum level of expression. The only difference between these two patterns is that peaks are shifted one-somite length posteriorly as each somite forms. Cells that end up in adjacent somites have opposite levels of clock expression in the anterior PSM, both temporally and spatially. This alternating pattern was recapitulated even when the clock was slowed using a *hes6* antisense morpholino, which has been previously shown to create larger somites (Schröter and Oates, 2010) (supplementary material Fig. S4).

DISCUSSION

Since the discovery of cyclic segmentation clock genes, researchers have explored how oscillations are translated to pattern future somites. Much of the work focuses on clock dynamics in the posterior PSM, where clock periodicity matches that of somite formation (Oates et al., 2012). Because a kinematic wave of clock expression narrows as it sweeps across the PSM, it is clear that the clock slows anteriorly (Giudicelli et al., 2007; Morelli et al., 2009; Ay et al., 2014). The gradual slowing of the clock has received less attention, largely due to the lack of real-time tools to measure changes in expression dynamics. We investigated how the longer clock period in the anterior PSM may influence forming somites.

Development (2015) 142, 1785-1793 doi:10.1242/dev.119057

Using an *in vivo* clock reporter, we examined clock expression in individual PSM cells as an embryo develops, correlating clock oscillations with morphological somite formation. We observed that segmentation clock periodicity and amplitude increases in the anterior PSM, with each wave of clock expression corresponding to a forming somite boundary. Our measurements of clock slowing match mathematical predictions made for the mouse (Niwa et al., 2011). The increase in amplitude may be due to a longer period, allowing for more protein to accumulate, though changes in expression or degradation rates may also play a role. A recent study has shown that increases in translational time of Her1 protein in the anterior PSM contribute to this slowing (Ay et al., 2014). Although it is not clear what regulates the change in cyclic gene expression dynamics in the anterior PSM, we know that *her1* expression in the anterior PSM is controlled by distinct regulatory elements (Gajewski et al., 2003; Brend and Holley, 2009), including a 500 bp upstream region with binding sites for Tbx24, Su(H) and Hairy-related transcriptional regulators (Brend and Holley, 2009). Additionally, signaling gradients, including FGF, Wnt and RA (Aulehla and Pourquié, 2010), could contribute to differential *her1* regulation in the anterior versus posterior PSM.

In vivo imaging of clock dynamics confirms that clock reporter expression gradually slows, with periodicity in the anterior PSM becoming almost double that in the posterior PSM. This periodicity creates an interesting phenomenon where at any given time in the anterior PSM, peaks of clock expression are spatially separated at a two-segment periodicity, with a trough of expression between them. After a round of somite formation, there are again two peaks of clock expression in the anterior PSM, shifted one-somite length compared with the previous two peaks, with the cells previously in the trough of expression now at a maximum (Fig. 3). In this way, there is an alternating two-segment periodicity, with each presumptive somite experiencing a peak of clock expression before boundary formation. As discussed later, this separation of clock expression peaks could be important in determining somite boundaries or defining anterior-posterior somite polarity. Clearly, real-time imaging is required to measure clock dynamics directly, and our study has elaborated, extended and refined what was previously inferred from studies in fixed embryos.

The slowing of the clock creates a spatial and temporal phase gradient, with expression marking two future alternating somites, with a gap of expression between them. This *in vivo* pattern mirrors previous fate mapping and *in situ* data: the distance between stripes of anterior PSM *her1* expression was measured to be up to two somites in length (Holley et al., 2000; Muller et al., 1996). Recent models of clock expression assert that expression peaks are separated by only one-somite length in the anterior-most PSM (Oates et al., 2012; Giudicelli et al., 2007; Morelli et al., 2009; Herrgen et al., 2010). The distance between each domain of segmentation gene expression differs among arthropods, with segmentation genes expressed at a one-segment length in spiders (Damen, 2007) or a two-segment length in insects such as beetles and fruit flies (Damen, 2007; Sarrazin et al., 2012). Our analyses show that peaks of clock expression in zebrafish differ depending upon position relative to the tailbud. Although *her1* is expressed as a dynamic kinematic wave, it is intriguing that *her1* spatial distribution in the anterior PSM at any given time has a similar alternating segment pattern to that of classic pair-rule genes (Muller et al., 1996; Nüsslein-Volhard and Wieschaus, 1980). The difference between classic pair-rule expression and what we observe, however, is that each future segment will alternate expression in the zebrafish anterior PSM, whereas only every other segment will ever express the classic pair-rule genes during *Drosophila* segmentation (Nüsslein-Volhard and Wieschaus, 1980).

In the original clock and wavefront model, the clock oscillates between a permissive and restrictive phase, interacting with the wavefront to mark distinct blocks of cells for somite formation (Cooke and Zeeman, 1976). One feature of this model is that somites can only be formed if groups of cells alternate between the permissive and restrictive phases of the clock. Later models incorporated additional features, such as the slowing of the clock. In these models, clock periodicity gradually increases to infinity at the PSM-somite boundary, with peaks of clock expression separated by one-segment length in the anterior PSM (Oates et al., 2012; Giudicelli et al., 2007; Herrgen et al., 2010; Morelli et al., 2009). We find that this does not accurately reflect key features of clock stopping, because such models predict that the clock period continuously diverges to infinity from anterior to posterior, with the anterior half of each presumptive somite ceasing oscillations before the posterior half. Because of the continuous change of period both within one somite and along the antero-posterior axis, we describe such models as 'wavefront stopping' models of clock oscillations. These models predict a smooth pattern of stopping in anterior, with a one-somite periodicity, and would be consistent with observations of the half-somite width of the anterior-most stripe of *her1* transcripts in a fixed embryo (Holley et al., 2000; Sawada et al., 2000) and on spacing of stripes in the anterior PSM (Giudicelli et al., 2007).

Our real-time imaging directly shows that the *her1:her1-Venus* clock reporter is not constantly expressed in the anterior half of the next presumptive somite. The half-somite stripe of clock gene expression observed in fixed embryos is likely the last part of the kinematic wave of clock expression sweeping through the PSM (Fig. 4A). Differences in interpretation may also be due to the focus on transcripts in fixed embryos, compared with protein levels in our *in vivo* experiments (cyclic transcripts and proteins have been shown to be expressed in offset domains) (Bessho et al., 2003; Takashima et al., 2011; Delaune et al., 2012; Giudicelli et al., 2007). We show that clock reporter expression in the anterior PSM is not restricted to any subset of cells; instead, all cells are oscillating, even at the PSM-somite boundary, so that the period does not increase gradually to infinity. Our reporter also revealed that within a future somite, presumptive posterior boundary cells cease oscillating before their anterior boundary counterparts (Fig. 4B), which is contrary to the classical view of a smooth posterior-progressing wavefront. We observe that cells cease oscillating with the same directionality as the waves of clock expression, consistent with the idea that the clock itself plays a role in determining the wavefront (Lauschke et al., 2013). We describe our model as 'clock wave stopping'. At the whole-tissue level, the clock stops from anterior to posterior, as observed with various real-time clock reporters (Lauschke et al., 2013; Aulehla et al., 2008; Masamizu et al., 2006; Takashima et al., 2011; Delaune et al., 2012; Soroldoni et al., 2014); however, within a given forming somite, clock stopping progresses from posterior to anterior. Thus, cells in each presumptive somite cease oscillating in discrete groups, rather than stopping in an anterior to posterior direction by a sweeping wavefront, as in the 'wavefront stopping' model (Fig. 4C). In our 'clock wave stopping' model, cells in the anterior PSM continue to oscillate with their neighbors, regardless of future somite position (Fig. 4C), consistent with the idea that synchrony is regulated by interactions between Delta-expressing and Notch-expressing cells (Delaune et al., 2012; Mara et al., 2007; Lewis, 2003; Horikawa et al., 2006; Riedel-Kruse et al., 2007;

Development (2015) 142, 1785-1793 doi:10.1242/dev.119057

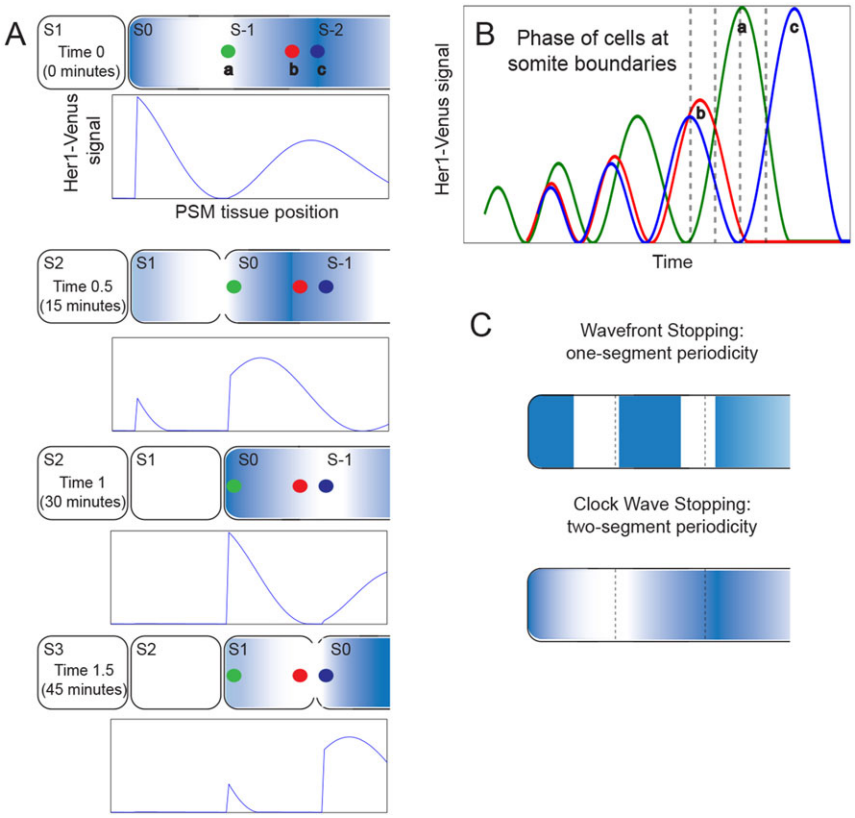

Fig. 4. A 'clock wave stopping' model of segmentation clock expression. (A) An idealized instantaneous phase of clock expression, with two representative time points shown for each somite formed. Blue shading indicates clock expression intensity, whereas white represents little or no clock expression. Diagrams under each embryo schematic show the expression pattern of the entire region at that timepoint. Colored dots represent the anterior boundary (green and blue) and posterior boundary (red) cells. Posterior boundary cells (red) stop oscillating long before adjacent anterior boundary cells (blue) reach their final peak, creating the sharp spatial drop of signal at each somite boundary. Half-somite regions of expression are shown in the anterior region of forming somites. (B) Clock expression of individual cells over time. Line color corresponds to cell position in A. Dashed lines indicate the time points shown in A-A‴. (C) Comparison of instantaneous phase pattern between 'wavefront stopping' models (Oates et al., 2012; Giudicelli et al., 2007; Morelli et al., 2009; Herrgen et al., 2010) and our revised 'clock wave stopping' model.

Özbudak and Lewis, 2008). Our data further suggest that a simple mechanism defining positional information could be at work. For example, as clock expression increases over the last two oscillations, levels may reach a threshold required to permanently repress its own expression and drive differentiation of PSM cells into a somite, which would explain the pattern of clock stopping we describe (Figs 2 and 4).

In a 'clock wave stopping' model, there is no requirement that the period of oscillations diverges to infinity to give rise to a smooth periodic one-somite pattern. Instead, the two-segment periodicity we observe might be crucial to sharply define antero-posterior polarity. With oscillation peaks at a two-somite length, cells in future adjacent somites are experiencing a maximal difference in clock expression, so that there is a clear polarity established within and between somites. Within one future somite, clock expression could then be, for example, discretized into anterior-posterior fates using a downstream bi-stable system (Meinhardt, 1982; François et al., 2007). This two-somite periodicity is preserved in the anterior PSM through the slowing of the clock, even though a wave of clock expression is generated in the posterior PSM every time one somite forms. Wavefront stopping models contend that peaks of expression in the anterior PSM are spaced at a one-somite periodicity, but we do not observe this in our study. What we observe instead – opposite phase at consecutive boundaries in the anterior PSM – reflects clock slowing and creates an alternating two-segment periodicity. The spatial two-segment periodicity not only makes it easier to distinguish consecutive boundaries due to their opposite phases, but has also been well described in other systems, such as *Drosophila*, the beetle *Tribolium* and mice (Niwa et al., 2011; Damen, 2007; Sarrazin et al., 2012). The correlation of gene oscillations and specific morphological landmarks may be a broad theme in development; for example, periodic expression of a cyclic reporter in *Arabidopsis* marks the future position of lateral root formation (Moreno-Risueno et al., 2010).

Heat-shock experiments and wavefront manipulations in zebrafish have suggested that boundary determination may occur as early as S-5 (Roy et al., 1999; Sawada et al., 2001; Akiyama et al., 2014). Experimental and modeling data have demonstrated that the sweeping wave of segmentation clock oscillations may not even be necessary for proper somite formation (Hester et al., 2010; Soza-Ried et al., 2014). Although initiation of somite patterning may occur in the posterior PSM, additional patterning mechanisms also operate later. For example, we have shown that a PSM cell dividing in S-3 can generate daughters that end up on opposite sides of a somite boundary, with appropriate oscillation profiles based on their final location (supplementary material Fig. S1). Conversely, local cell rearrangements can separate cells that were originally neighbors and are similarly fated; cell tracking work has shown that some PSM cells apparently switch sides right before boundaries form (Henry et al., 2000). Similarly, time-lapse analyses of neural tube patterning show that cell-type specification occurs early, but is spatially irregular; local rearrangements then sort like cells together (Xiong et al., 2013). Signals in the posterior PSM clearly have an important role in determining boundary formation, but our observations suggest that the final boundary decision is refined in the anterior PSM. Manipulating oscillations in different PSM regions will resolve whether the oscillatory changes we observe influence somite fate, or are an output of the fate decision. We note that our model is based only on observations of Her1 oscillatory expression and do not include other segmentation clock components. Future experiments in the zebrafish segmentation clock system will clarify the role of other PSM genes in distinguishing and separating PSM cells into discrete somites.

As we continue to investigate somitogenesis, more sophisticated analytical tools will expand our understanding of the underlying mechanisms. Our findings have revealed complex behaviors of the segmentation clock and how the clock may play a more central role in segmenting boundaries. The slowing of the clock in the anterior PSM

Development (2015) 142, 1785-1793 doi:10.1242/dev.119057

is precise, generating separation of phase both temporally and spatially. Real-time reporters are important to capture dynamics not otherwise observable, and will continue to enhance our understanding of the segmentation clock.

MATERIALS AND METHODS

Fish husbandry

Adult fish strains were kept at 28.5°C on a 14 h-light/10 h-dark cycle. Embryos were obtained by natural crosses or *in vitro* fertilization, and staged via established criteria (Kimmel et al., 1995). The Tg(*her1:her-Venus*)^{bk15} transgenic line has been described previously (Delaune et al., 2012) and consists of *her1* gene cyclic regulatory elements driving expression of a Her1-Venus fusion protein. All imaging experiments were performed in embryos heterozygous for the transgene, obtained by crossing fish homozygous for the transgene to the wild-type AB strain. Animal experiments were performed in accordance with institutional and national guidelines, and regulations and were approved by the UC Berkeley and Ohio State University Animal Care and Use Committees.

Live imaging

Time-lapse images were generated using methods modified from Delaune et al. (2012). Embryos were imaged on a LSM 780 with 32-channel GaAsP detector on the AxioExaminer microscope (Carl Zeiss) with the W Plan-Apochromat 20×/1.0 NA objective (Carl Zeiss), using Zeiss Zen 2010 software. Owing to low level fluorescence, we have found that the numerical aperture of the objective is a crucial component. Confocal sections were taken every 2 µm, with a stack of 30-35 slices taken approximately every 4 min. Images were converted to 8-bit tagged image file format before processing.

3D cell contour detection and tracking

Semi-automated contour detection MATLAB scripts were used to segment individual cells, as described previously (Delaune et al., 2012). As in our previous work, automated tracking of all individual cells was manually corrected and validated before further analyses.

Phase smoothing and phase calculation

A sine wave for each cell was generated using a smoothing heuristic, as described previously (Delaune et al., 2012). The phase at each timepoint was then extrapolated based on the smoothed sine wave. The extrapolated phase of a cell at a particular timepoint was compared with the phase of other cells at the same timepoint, and the absolute values for these phase differences were plotted onto histograms.

Tissue-wide partitioning and fluorescence binning

Cell positions and contours in the developing embryos were detected based on nuclear and membrane fluorescence within each *z*-stack. Image stacks were treated with low-pass filters to remove background and noise (Delaune et al., 2012). A binary image was constructed to detect embryo contour and to compute a skeleton corresponding to the center axis. We then defined a curved coordinate along this axis, and computed the position of each cell along this coordinate. This reference axis was then partitioned into equal parts, with the extended segment boundaries corresponding to bins. Fluorescence within each slice was measured as an average compared with slice size, and stored based on tissue position and timepoint. Embryo movement was accounted for by anchoring tissue position to a known reference cell as a landmark.

Acknowledgements

We thank the UC Berkeley and Ohio State Zebrafish Facilities staff for excellent zebrafish care. We thank Holly Aaron, Samuel Coleman, the UC Berkeley Molecular Imaging Center and the OSU Neuroscience Imaging Core for confocal access and advice, and Susan Cole for reviewing the manuscript. N.P.S. thanks Craig Miller, David Weisblat, and Patricia Zambryski for their invaluable input and feedback, and Paul Wang for excellent technical assistance.

Competing interests

The authors declare no competing or financial interests.

Author contributions

N.P.S. performed timelapse imaging and cell tracking experiments, which were conceived and designed by all authors. MATLAB-based computer analyses and modeling were performed by N.P.S. and P.F. N.P.S., E.A.D. and S.L.A. provided reagents and materials. All authors contributed intellectually and discussed the data and manuscript. N.P.S., P.F. and S.L.A. wrote the manuscript and all authors participated in the editing process.

Funding

The work was funded by the Association Française contre les Myopathies (E.A.D.), a Marie Curie Outgoing International Fellowship (E.A.D.) and an National Institutes of Health (NIH) grant [1-R01-GM061952 to S.L.A.], supplemented by the American Recovery and Reinvestment Act. P.F. is supported by the Natural Science and Engineering Research Council of Canada, Discovery Grant program, Fonds de recherche du Québec – Nature et technologies, and partially supported by the Human Frontier Science Program and a Simons Foundation Investigator Award in the Mathematical Modeling of Living Systems. N.P.S. was supported by an NIH Training Grant [GM007127]. Deposited in PMC for release after 12 months.

Supplementary material

Supplementary material available online at
http://dev.biologists.org/lookup/suppl/doi:10.1242/dev.119057/-/DC1

References

Akiyama, R., Masuda, M., Tsuge, S., Bessho, Y. and Matsui, T. (2014). An anterior limit of FGF/Erk signal activity marks the earliest future somite boundary in zebrafish. *Development* **141**, 1104-1109.

Aulehla, A. and Pourquié, O. (2010). Signaling gradients during paraxial mesoderm development. *Cold Spring Harb. Perspect. Biol.* **2**, a000869.

Aulehla, A., Wiegraebe, W., Baubet, V., Wahl, M. B., Deng, C., Taketo, M., Lewandoski, M. and Pourquié, O. (2008). A beta-catenin gradient links the clock and wavefront systems in mouse embryo segmentation. *Nat. Cell Biol.* **10**, 186-193.

Ay, A., Holland, J., Sperlea, A., Devakanmalai, G. S., Knierer, S., Sangervasi, S., Stevenson, A. and Ozbudak, E. M. (2014). Spatial gradients of protein-level time delays set the pace of the traveling segmentation clock waves. *Development* **141**, 4158-4167.

Bessho, Y., Sakata, R., Komatsu, S., Shiota, K., Yamada, S. and Kageyama, R. (2001). Dynamic expression and essential functions of Hes7 in somite segmentation. *Genes Dev.* **15**, 2642-2647.

Bessho, Y., Hirata, H., Masamizu, Y. and Kageyama, R. (2003). Periodic repression by the bHLH factor Hes7 is an essential mechanism for the somite segmentation clock. *Genes Dev.* **17**, 1451-1456.

Brend, T. and Holley, S. A. (2009). Expression of the oscillating gene her1 is directly regulated by Hairy/Enhancer of Split, T-box, and Suppressor of Hairless proteins in the zebrafish segmentation clock. *Dev. Dyn.* **238**, 2745-2759.

Cooke, J. and Zeeman, E. C. (1976). A clock and wavefront model for control of the number of repeated structures during animal morphogenesis. *J. Theor. Biol.* **58**, 455-476.

Damen, W. G. M. (2007). Evolutionary conservation and divergence of the segmentation process in arthropods. *Dev. Dyn.* **236**, 1379-1391.

Delaune, E. A., François, P., Shih, N. P. and Amacher, S. L. (2012). Single-cell-resolution imaging of the impact of Notch signaling and mitosis on segmentation clock dynamics. *Dev. Cell* **23**, 995-1005.

François, P. and Siggia, E. D. (2012). Phenotypic models of evolution and development: geometry as destiny. *Curr. Opin. Genet. Dev.* **22**, 627-633.

François, P., Hakim, V. and Siggia, E. D. (2007). Deriving structure from evolution: metazoan segmentation. *Mol. Syst. Biol.* **3**, 154.

Gajewski, M., Sieger, D., Alt, B., Leve, C., Hans, S., Wolff, C., Rohr, K. B. and Tautz, D. (2003). Anterior and posterior waves of cyclic her1 gene expression are differentially regulated in the presomitic mesoderm of zebrafish. *Development* **130**, 4269-4278.

Giudicelli, F., Özbudak, E. M., Wright, G. J. and Lewis, J. (2007). Setting the tempo in development: an investigation of the zebrafish somite clock mechanism. *PLoS. Biol.* **5**, e150.

Henry, C. A., Hall, L. A., Burr Hill, M., Solnica-Krezel, L. and Cooper, M. S. (2000). Somites in zebrafish doubly mutant for knypek and trilobite form without internal mesenchymal cells or compaction. *Curr. Biol.* **10**, 1063-1066.

Henry, C. A., Urban, M. K., Dill, K. K., Merlie, J. P., Page, M. F., Kimmel, C. B. and Amacher, S. L. (2002). Two linked hairy/Enhancer of split-related zebrafish genes, her1 and her7, function together to refine alternating somite boundaries. *Development* **129**, 3693-3704.

Herrgen, L., Ares, S., Morelli, L. G., Schröter, C., Jülicher, F. and Oates, A. C. (2010). Intercellular coupling regulates the period of the segmentation clock. *Curr. Biol.* **20**, 1244-1253.

Hester, S. D., Belmonte, J. M., Gens, S. J., Clendenon, S. G. and Glazier, J. A. (2010). A multi-cell, multi-scale model of vertebrate segmentation and somite formation. *PLoS Comput. Biol.* **10**, e1002155.
Holley, S. A., Geisler, R. and Nusslein-Volhard, C. (2000). Control of her1 expression during zebrafish somitogenesis by a delta-dependent oscillator and an independent wave-front activity. *Genes Dev.* **14**, 1678-1690.
Horikawa, K., Ishimatsu, K., Yoshimoto, E., Kondo, S. and Takeda, H. (2006). Noise-resistant and synchronized oscillation of the segmentation clock. *Nature* **441**, 719-723.
Jiang, Y.-J., Aerne, B. L., Smithers, L., Haddon, C., Ish-Horowicz, D. and Lewis, J. (2000). Notch signalling and the synchronization of the somite segmentation clock. *Nature* **408**, 475-479.
Jouve, C., Palmeirim, I., Henrique, D., Beckers, J., Gossler, A., Ish-Horowicz, D. and Pourquié, O. (2000). Notch signalling is required for cyclic expression of the hairy-like gene HES1 in the presomitic mesoderm. *Development* **127**, 1421-1429.
Jülich, D., Hwee Lim, C., Round, J., Nicolaije, C., Schroeder, J., Davies, A., Geisler, R., Lewis, J., Jiang, Y.-J. and Holley, S. A. (2005). beamter/deltaC and the role of Notch ligands in the zebrafish somite segmentation, hindbrain neurogenesis and hypochord differentiation. *Dev. Biol.* **286**, 391-404.
Kimmel, C. B., Ballard, W. W., Kimmel, S. R., Ullmann, B. and Schilling, T. F. (1995). Stages of embryonic development of the zebrafish. *Dev. Dyn.* **203**, 253-310.
Lauschke, V. M., Tsiairis, C. D., François, P. and Aulehla, A. (2013). Scaling of embryonic patterning based on phase-gradient encoding. *Nature* **493**, 101-105.
Lewis, J. (2003). Autoinhibition with transcriptional delay: a simple mechanism for the zebrafish somitogenesis oscillator. *Curr. Biol.* **13**, 1398-1408.
Lewis, J., Hanisch, A. and Holder, M. (2009). Notch signaling, the segmentation clock, and the patterning of vertebrate somites. *J. Biol.* **8**, 44.
Mara, A., Schroeder, J., Chalouni, C. and Holley, S. A. (2007). Priming, initiation and synchronization of the segmentation clock by deltaD and deltaC. *Nat. Cell Biol.* **9**, 523-530.
Masamizu, Y., Ohtsuka, T., Takashima, Y., Nagahara, H., Takenaka, Y., Yoshikawa, K., Okamura, H. and Kageyama, R. (2006). Real-time imaging of the somite segmentation clock: revelation of unstable oscillators in the individual presomitic mesoderm cells. *Proc. Natl. Acad. Sci. USA* **103**, 1313-1318.
Megason, S. G. (2009). In toto imaging of embryogenesis with confocal time-lapse microscopy. *Methods Mol. Biol.* **546**, 317-332.
Meinhardt, H. (1982). *Models of Biological Pattern Formation*. London, UK: Academic Press.
Morelli, L. G., Ares, S., Herrgen, L., Schröter, C., Jülicher, F. and Oates, A. C. (2009). Delayed coupling theory of vertebrate segmentation. *HFSP J.* **3**, 55-66.
Moreno-Risueno, M. A., Van Norman, J. M., Moreno, A., Zhang, J., Ahnert, S. E. and Benfey, P. N. (2010). Oscillating gene expression determines competence for periodic Arabidopsis root branching. *Science* **329**, 1306-1311.
Muller, M., Weizsacker, E. v. and Campos-Ortega, J. A. (1996). Expression domains of a zebrafish homologue of the Drosophila pair-rule gene hairy correspond to primordia of alternating somites. *Development* **122**, 2071-2078.
Niwa, Y., Shimojo, H., Isomura, A., Gonzalez, A., Miyachi, H. and Kageyama, R. (2011). Different types of oscillations in Notch and Fgf signaling regulate the spatiotemporal periodicity of somitogenesis. *Genes Dev.* **25**, 1115-1120.
Nüsslein-Volhard, C. and Wieschaus, E. (1980). Mutations affecting segment number and polarity in Drosophila. *Nature* **287**, 795-801.
Oates, A. C. and Ho, R. K. (2002). Hairy/E(spl)-related (Her) genes are central components of the segmentation oscillator and display redundancy with the Delta/Notch signaling pathway in the formation of anterior segmental boundaries in the zebrafish. *Development* **129**, 2929-2946.
Oates, A. C., Morelli, L. G. and Ares, S. (2012). Patterning embryos with oscillations: structure, function and dynamics of the vertebrate segmentation clock. *Development* **139**, 625-639.
Özbudak, E. M. and Lewis, J. (2008). Notch signalling synchronizes the zebrafish segmentation clock but is not needed to create somite boundaries. *PLoS Genet.* **4**, e15.
Palmeirim, I., Henrique, D., Ish-Horowicz, D. and Pourquié, O. (1997). Avian hairy gene expression identifies a molecular clock linked to vertebrate segmentation and somitogenesis. *Cell* **91**, 639-648.
Pourquié, O. (2011). Vertebrate segmentation: from cyclic gene networks to scoliosis. *Cell* **145**, 650-663.
Pourquié, O. and Tam, P. P. L. (2001). A nomenclature for prospective somites and phases of cyclic gene expression in the presomitic mesoderm. *Dev. Cell* **1**, 619-620.
Riedel-Kruse, I. H., Muller, C. and Oates, A. C. (2007). Synchrony dynamics during initiation, failure, and rescue of the segmentation clock. *Science* **317**, 1911-1915.
Roy, M. N., Prince, V. E. and Ho, R. K. (1999). Heat shock produces periodic somitic disturbances in the zebrafish embryo. *Mech. Dev.* **85**, 27-34.
Sarrazin, A. F., Peel, A. D. and Averof, M. (2012). A segmentation clock with two-segment periodicity in insects. *Science* **336**, 338-341.
Sawada, A., Fritz, A., Jiang, Y. J., Yamamoto, A., Yamasu, K., Kuroiwa, A., Saga, Y. and Takeda, H. (2000). Zebrafish Mesp family genes, mesp-a and mesp-b are segmentally expressed in the presomitic mesoderm, and Mesp-b confers the anterior identity to the developing somites. *Development* **127**, 1691-1702.
Sawada, A., Shinya, M., Jiang, Y. J., Kawakami, A., Kuroiwa, A. and Takeda, H. (2001). Fgf/MAPK signaling is a crucial positional cue in somite boundary formation. *Development* **128**, 4873-4880.
Schröter, C. and Oates, A. C. (2010). Segment number and axial identity in a segmentation clock period mutant. *Curr. Biol.* **20**, 1254-1258.
Schröter, C., Herrgen, L., Cardona, A., Brouhard, G. J., Feldman, B. and Oates, A. C. (2008). Dynamics of zebrafish somitogenesis. *Dev. Dyn.* **237**, 545-553.
Soroldoni, D., Jörg, D. J., Morelli, L. G., Richmond, D. L., Schindelin, J., Jülicher, F. and Oates, A. C. (2014). Genetic oscillations. A Doppler effect in embryonic pattern formation. *Science* **345**, 222-225.
Soza-Ried, C., Öztürk, E., Ish-Horowicz, D. and Lewis, J. (2014). Pulses of Notch activation synchronise oscillating somite cells and entrain the zebrafish segmentation clock. *Development* **141**, 1780-1788.
Takashima, Y., Ohtsuka, T., Gonzalez, A., Miyachi, H. and Kageyama, R. (2011). Intronic delay is essential for oscillatory expression in the segmentation clock. *Proc. Natl. Acad. Sci. USA* **108**, 3300-3305.
Xiong, F., Tentner, A. R., Huang, P., Gelas, A., Mosaliganti, K. R., Souhait, L., Rannou, N., Swinburne, I. A., Obholzer, N. D., Cowgill, P. D. et al. (2013). Specified neural progenitors sort to form sharp domains after noisy Shh signaling. *Cell* **153**, 550-561.